

On the Evaluation of SEEs on Open-Source Embedded Static RAMs

Original

On the Evaluation of SEEs on Open-Source Embedded Static RAMs / Azimi, Sarah; De Sio, Corrado; Sterpone, Luca. - ELETTRONICO. - (2021), pp. 1-6. (Intervento presentato al convegno IEEE International Conference on Very Large Scale Integration (VLSI-SoC) nel 4-7 October 2021) [10.1109/VLSI-SoC53125.2021.9606985].

Availability:

This version is available at: 11583/2923841 since: 2022-04-13T15:30:34Z

Publisher:

IEEE

Published

DOI:10.1109/VLSI-SoC53125.2021.9606985

Terms of use:

This article is made available under terms and conditions as specified in the corresponding bibliographic description in the repository

Publisher copyright

IEEE postprint/Author's Accepted Manuscript

©2021 IEEE. Personal use of this material is permitted. Permission from IEEE must be obtained for all other uses, in any current or future media, including reprinting/republishing this material for advertising or promotional purposes, creating new collecting works, for resale or lists, or reuse of any copyrighted component of this work in other works.

(Article begins on next page)

On the Evaluation of SEEs on Open-Source Embedded Static RAMs

S. Azimi, C. De Sio, L. Sterpone
Dipartimento di Automatica e Informatica
Politecnico di Torino
Torino, Italy
{sarah.azimi, corrado.desio, luca.sterpone}@polito.it

Abstract— Static RAM modules are widely adopted in high performance systems. Single Event Effects (SEEs) resilient memories are required in many embedded systems applied in automotive and aerospace applications to increase their overall resiliency against SEEs. The current SEE resilient SRAM modules are obtained by applying radiation-hardened by design solutions which leads to elevated area overhead and difficulty to tune the resiliency capability with respect to the particle’s radiation profile. To overcome these limitations, we propose a methodology for the analysis and mitigation of embedded SRAMs generated by the OpenRAM memory compiler. A technology-oriented radiation analysis tool is presented to support the interaction of the charged radiation particles with the SRAM layout and depict the sensitive transistors of the SRAM memory. A selective duplication of the sensitive transistors has been applied to the 6T-SRAM cell designed at the layout level. The designed cell is included in the OpenRAM compiler and used to generate a mitigated 8Kb SRAM-bank. We evaluated the SEEs sensitivity by comparative simulation-based radiation analysis observing a reduction more than 6 times with respect to the original 6T-SRAM cell for the SEE sensitivity at high energy heavy ions particles, with negligible degradation of operations margins and power consumption and area overhead of less than-4%.

I. INTRODUCTION

EMBEDDED Static Random Access Memories are widely applied in various kinds of commercial applications and they are today an integrated module of aerospace and automotive microprocessor systems [1]. RAMs are crucial components in System-on-chips (SoCs) and due to their wide application, SRAM modules are characterized by several memory configuration requirements and constraints especially when they are adopted in harsh environments [2]. SRAMs are vulnerable to two main effects, on one side they are really sensitive to wear-out mechanisms such as aging, where the Bias Temperature Instability (BTI) has been discovered as the main reliability concern. On the other side, SRAM cells are extremely sensitive to radiation-induced errors such as Single Event Effects (SEEs) caused by charged particles passing through the semiconductor device and generating electron-hole pairs along the particle track. The collected charge (Q_{coll}) of electron-hole pairs may change the memory cell state in the case it is greater than the critical charge (Q_{crit}) [3]. The radiation sensitivity of embedded SRAM is more emphasized considering that the area used by SRAM memory is dominating

the physical layout of CPUs or GPUs [3]. Hence, SRAM layout is typically characterized by minimum device geometry that tends to reduce the Q_{crit} and conversely increase the sensitivity to radiation-induced errors. In order to manufacture robust SRAM modules and to increase the immunity to SEE, design and mitigation strategies for SRAM apply radiation-hardened-by-design (RHBD) that are generally adopting special epitaxial or eventually SOI substrate to limit ionizing radiation particle track length and including high-density capacitors and resistors to avoid circuit response to the collected charge [4]. Since the elevated cost of RHBD, typically error detection and correction (EDAC) approaches are applied to SRAM modules such as caches and shared memory [5]. However, the inclusion of extra combinational logic, such as the one used for Error Correction Mechanism, may also increase the occurrences of Single Event Transients (SETs) since these errors are not easily protected by EDAC.

Considering the growing role of embedded SRAM in system performances, several memory compiler tools have been recently developed [6]. The need for these tools was supported by the fact that most academic ICs design approaches are limited by the effective availability of memories. Nowadays, with the advent of an open-source customizable compiler, researchers are able to design their own memory module with the proper regular structure and configuration. This represents an undoubted advantage in hardware design since the basic building blocks are provided by foundries in technology process design kits (PDKs) and they are essential for hardware and device realization [7]. Thanks to the availability of open-source PDKs for RAMs, several researchers recently started to investigate the applicability of reliability analysis and mitigation of open-source hardware designs [8].

In this work, we propose a new analysis and mitigation framework targeting the Single Event Effects (SEE) radiation-induced phenomena on Open-RAM physical design. The OpenRAM project is an open-source memory compiler freely available under BSC license [6]. The compiler may be used for the design of new architectures in order to evaluate power, performances and area overhead on the other side, OpenRAM is usable to prototype and evaluate technological modification [9] We selected Cyclone, the cyclotron of the University Catholic the Louvain (UCL) heavy ions high-penetration cocktail as a reference for the radiation characterization. We

perform a complete radiation sensitivity evaluation of the RAM block core cells in order to individuate the SEE cross-section and potential weak points of each memory component. Secondly, we apply selective mitigation solutions to the 6T cell of the SRAM by hardening the most sensitive transistor. The hardening insertion has been automatized by the development of a tool to manipulate the physical layout of each cell and to insert a resized duplicated transistor into the 6T cell physical layout structure capable to increase the critical charge of the 6T cell structure.

This work has two main scientific contributions. The former is characterized by the first heavy ions radiation sensitivity evaluation of open-source embedded RAMs showing promising results and a large margin of improvements. The second is the realization of a tool to manipulate physical layout on large scale and to introduce mitigation strategies, the tool may be also ported to commercial technology nodes using library technology files. In order to evaluate the developed methodology, we designed two memory blocks using the physical implementations at 45nm technology with the OpenRAM compiler adopting the FreePDK45 design kit and we performed comparative simulation-based radiation analysis. Experimental results demonstrate that the mitigated OpenRAM memory is approximately 35% more robust than the original OpenRAM design with a marginal degradation of the circuit performance and an area overhead of less than 4%.

This paper is organized as follows. Section II presents previous works related to analysis and mitigation methods for SEE effects on SRAM modules. Section III gives an overview on the OpenRAM analysis method, while the mitigation approach is described in Section IV. The experimental results are reported in Section V. Finally, Section VI drafts some conclusions and future works.

II. RELATED WORKS

Several previous works have already analyzed the impact of radiation particles on SRAM cells. With the progressive technology scaling, the amount of errors within SRAM module drastically increases. This effect can be explained by both the SRAM cell junction reduction and by the reduced space between cells and lower values of critical charge [9][10]. Radiation tests and 3-D simulations already demonstrated that the bipolar parasitic physical mechanism of the MOS transistors is activated by radiation particle strikes and is the cause of memory upsets [11]. In the last decade, real-time radiation test explored the sensitivity of 45nm SRAM modules and identify the soft error projection with respect to the type of radiation particles and energies. The obtained results demonstrated the importance of the device manufacturing and the thick interconnect metallization and dielectric layers with respect to the effective sensitivity to charged particles [12].

On the other hand, two main categories of mitigation techniques targeting the corrections of single and multiple cell upsets were proposed. The first category relies on the insertion of Error Correction Code (ECC) mechanisms at the architectural level, while effective for Single Event Upsets (SEUs) these approaches are not able to cope with a large

number of Multiple Event Upsets (MEUs), usually happening in the same word and not necessarily in adjacent cells [13]. Besides, traditional error detection and correction approaches introduce critical timing on memory access making these solutions difficultly applicable in cache memories [14].

The second category is based on radiation-hardened-by-design (RHBD) techniques that allows to apply radiation mitigation circuit solutions to the manufacturing process of commercial foundries in order to minimize the impact of radiation particles [15]. The main focus of RBHD techniques have been on Single Event Upsets (SEUs) affecting the 6T-SRAM cell. The developed mitigation solutions were based on resizing of the sensitive transistors [16] or adding extra transistors to reduce the proximity of the radiation strike and distribute the charge collection. The insertion of extra transistors to the original 6T-RAM cell has been also provided in the 8T-SRAM [17] where two transistors are added to eliminate the charge sharing effect between the bit lines or in the differential-ended 10T-SRAM [18] for increasing the speed of the bit line signal or even as 12T-SRAM to reduce the noise disturbance of the bit cell interleaving structure.

In this work, we investigate specifically the sensitivity and mitigation of recoverable SEEs phenomena affecting a SRAM memory bank. Typically, this type of SEE effect happens in ground and avionics applications or, for aerospace applications at Low Earth Orbit (LEO), where the eventuality of ultra-high energy radiation particle is nullified by the Earth magnetic field. Thanks to the layout-oriented radiation analysis we implement a RHBD mitigation solution at the layout level increasing the robustness of the original 6T-SRAM cell by adding two parametrizable transistors that can be tunable with respect to the radiation particle energy required.

III. THE 45NM TECHNOLOGY RADIATION ANALYSIS

In order to achieve an accurate radiation sensitivity of the SRAM module, we developed the radiation particle simulation environment illustrated in Figure 1. The simulation flow is based on the 3D radiation particle propagation tool presented in [20] and available as open-source code. We extracted the physical layout description of the OpenRAM basic cell library and we inserted the layer material, thickness and depth to the Graphic Data Systems (GDS) description.

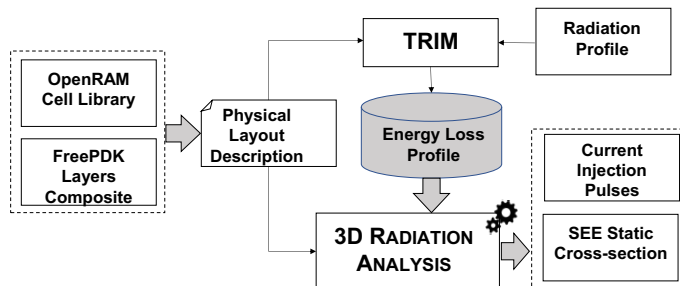


Fig. 1. The developed 3D simulation for the radiation particle analysis on the OpenRAM cell library layout geometry.

The physical description and the particle radiation profile generated by the Transport of Ions in Matter (TRIM) tool are

used to calculate the energy distribution released by the ions traversing the layer section of the cell. The last step of the analysis consists on the analysis of the physical layout description and the energy loss of the radiation particle used to calculate the transient sensitivity of the logic cells in terms of SEE cross-section and the correspondent current injection pulses generated within the cell geometry.

A. The FreePDK45nm technology node

The OpenRAM memory module is generated by the open-source compiler using the open-source variation-aware physical design kit FreePDK [19] based on Scalable CMOS design rules. The cell library includes variation-aware tools compatible with commercial design tools based on a theoretical 45nm technology where each cell is described by a proper structure including rectangular vias, metalizations and interconnects as well as silicon active regions. We integrated the FreePDK library information building a 3D model of the cell library adding thickness and layer material adopting the modeling provided by the 45nm high performance bulk logic platform technology lithography [21]. The generated model consists on 13 layers from the Active region, the Well and implant sections up to three aluminum metalizations connected by copper vias. The data of the generated model are represented in Table I while a structural view of a 6T-SRAM cell of the OpenRAM module is illustrated in Fig. 2.

TABLE I
45NM FREEPDK LAYERS, THICKNESS AND COMPOSITE MATERIAL

| Layer Name | Layer [#] | Thickness [nm] | Layer Material |
|--------------|-----------|----------------|--------------------------------|
| Active | 1 | 520 | SiO ₂ |
| N-Well | 2 | 100 | n-Si |
| P-Well | 3 | 110 | p-Si |
| N-implant | 4 | 100 | n-Si |
| P-implant | 5 | 110 | p-Si |
| S-Block | 6 | 85 | SiN |
| Poly-Silicon | 9 | 85 | Poly-Si |
| Contact | 10 | 150 | Si ₃ N ₄ |
| M1 | 11 | 130 | Al |
| Via1 | 12 | 120 | Cu |
| M2 | 13 | 140 | Al |
| Via2 | 14 | 120 | Cu |
| M3 | 15 | 140 | Al |

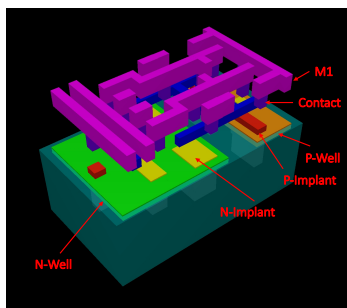


Fig. 2. The 45nm 6T-SRAM cell 3D model view from the Active layer up to the metallization M1.

The size of each layer and the position of each volumetric region of the FreePDK library has been modeled considering the thickness and the implant position in order to achieve a compliant three dimensional model.

B. SEE Radiation Analysis

The radiation analysis is performed considering four heavy ions energy profile related to the UCL facility [22]. Table II reports the energies, ion range and Linear Energy Transfer (LET) used. The analysis starts by extracting the geometry and size data of layer volumes, material composition as well as the radiation profile for the considered particles. The TRIM application calculate the energy loss level of the particle for each layer of the cell. Fig. 3 represents the amount of released energy in each layer of the cell considering the *Aluminium* and *Xenon* heavy ion particles at the energies defined in Table II. Interestingly, *vias* are the volumes with the highest value of energy loss, while the metalizations, contacts and in implants and well have a low energy loss.

TABLE II
RADIATION PARTICLE CHARACTERISTICS

| Ion | DUT Energy [MeV] | Range [μ mSi] | LET [MeV/mg/cm ²] |
|----------------------------------|------------------|--------------------|-------------------------------|
| ¹³ C ⁴⁺ | 131 | 269.3 | 1.3 |
| ²⁷ Al ¹⁸⁺ | 250 | 131.2 | 5.7 |
| ⁵⁸ Ni ¹⁸⁺ | 582 | 100.5 | 20.4 |
| ¹²⁴ Xe ³⁵⁺ | 995 | 73 | 62.5 |

The developed tool elaborates the physical description of the cell, generating the 3D mesh structure of the layout of the logic cell. Based on the size, shape, and material of metallization and volumes of the cell with respect to the radiation profile of the mission represented in Table II, the developed radiation analysis tool simulates the effects of highly charged particles traversing the silicon junction of the device and calculate the generated eV transmitted to the Silicon matter by the particles and provide the current profile for each particle strike.

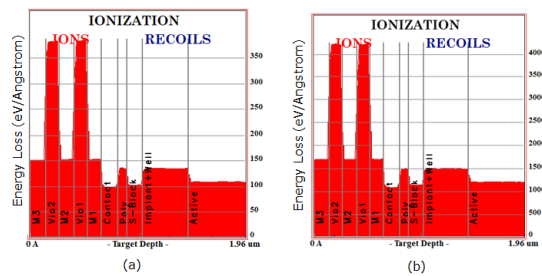


Fig. 3. Released Energy profile for the different layers of the 45nm cell for the Aluminum (a) and the Xenon (b) energy levels.

C. OpenRAM radiation sensitivity

An OpenRAM module consists in eight blocks as illustrated in the overall scheme in Fig. 4. The hierarchical blocks of the memory bank are based on six main logic cells: Data Flip-Flop (DFF), Master and Slave Flip-Flip (MS-Flop), Write Drivers, Three states buffer, Sense Amplifier and the 6 Transistors RAM cell. The hierarchical decoder and the control logic gates are outside of the memory bank, however they are mainly based on DFFs and combinational logic cells which radiation sensitivity can be determined with traditional analysis method [25] We analyzed the memory bank cells with 10,000 heavy ions particle using the 3D simulation approach and we computed the SEE cross-section for each cell. The results are illustrated in Fig. 5. The SEE cross-section may vary from $5.44 \cdot 10^{-14}$ up to $5.46 \cdot 10^{-14}$.

¹³. The DFFs and the MS-Flops are the most sensitive cells while the 6T-DRAM cell is interestingly the cell with the lower cross-section curve. However, considering the number of cells per block, the memory bank cross-section is fully determined by the sensitivity of the 6T-SRAM cell. For example, considering a memory bank of 8Kb, the cross-section is equivalent to $1.43 \cdot 10^{-9}$ totally due by the 6T-SRAM radiation sensitivity.

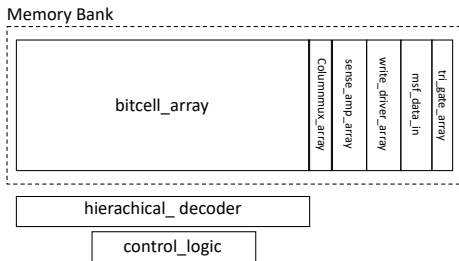


Fig. 4. The overall OpenRAM hierarchical blocks. The hierarchical decoder and control logic modules are outside from the memory bank.

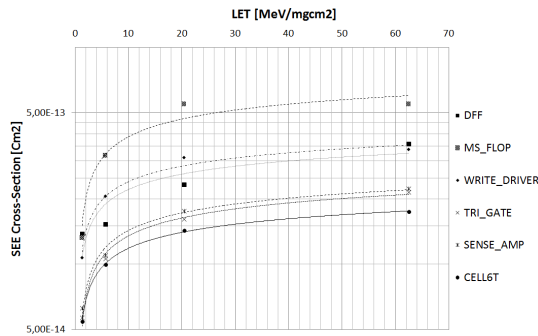


Fig. 5. The Single Event Effects (SEEs) cross-section sensitivity for the OpenRAM memory bank individual cell components.

We performed a Monte Carlo analysis in order to depict the vulnerability regions of the 6T-SRAM cells and individuating the parasitic thyristor resistance spectrum distribution on the cell layout considering a static and unpowered condition of the cell. In Fig. 6, it is possible to observe that the SRAM has various sensitive area, most of them correlated to the layout position of the 6 transistors. Besides, we calculated the distribution of the current pulses observing that 96.62% of the radiation particle injected over the 40,000 injection performed by the selected ions are generating current pulse below $0.5 \mu\text{A}$ with a maximal peak of $17.4 \mu\text{A}$.

IV. 8T-SRAM MITIGATION STRATEGIES

Traditional 8T-SRAM schemes are based on the insertion of 2 additional transistors to the 6T scheme depending on the target application of the memory. In case of mitigation solutions for soft-errors, extra transistors are generally added to introduce redundancy to the bit-lines or to the NMOS and PMOS used to implement the SRAM storage. The main purpose of our approach is to insert two redundant transistors in parallel to the original PMOS transistors, in order to distribute the radiation particle charge injected by those particles directly crossing MP5 and MP6 and to increase the overall Q_{crit} margins for the transient effects introduced by particles crossing other regions of the cell.

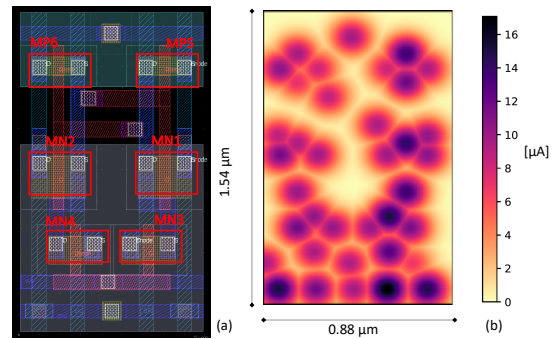


Fig. 6. The 6T-SRAM layout (a) and the vulnerability region reporting the μA current spectrum for the Xenon energy analysis on the overall area (b).

We adopted a different approach to insert the redundant transistors to the original scheme. Thanks to the availability of the OpenRAM layout, instead to start the mitigation insertion from the electrical scheme, we considered at first the 6T-SRAM original layout available regions that can be modified without introducing area overhead to the cell. We identify on the top of the MP6 and MP5 transistors enough physical space to introduce to redundant transistors without affecting the SRAM cell size.

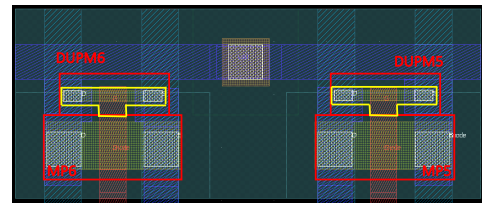


Fig. 7. The view of the top area of the SRAM cell including the duplicated transistor T structure, highlighted in yellow.

We introduced the following layers for each transistor: an active layer with $h=0.02 \mu\text{m}$ and $w=0.19 \mu\text{m}$; a P-implant layer with $h=0.02 \mu\text{m}$ and $w=0.18 \mu\text{m}$ centered with respect to the active layer; the poly-silicon section vertical to the active layer has been extended of $0.05 \mu\text{m}$ in order to be effective with respect to the active layer; two contact regions of $h=0.02 \mu\text{m}$ and $w=0.035 \mu\text{m}$, finally, we extended the metallization M1 of $0.06 \mu\text{m}$ in order to connect properly the VDD source and the drain and source junctions.

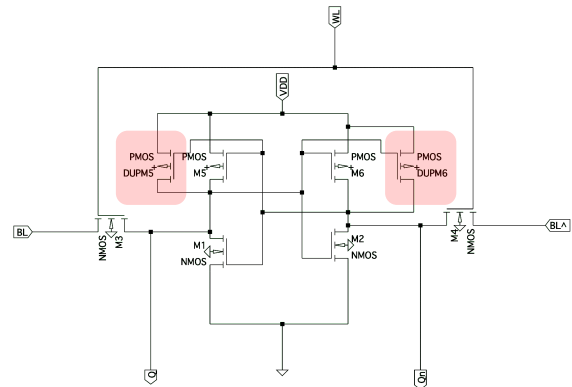


Fig. 8. The electrical scheme obtained from the layout technology extraction of the mitigated 8T-SRAM cell with the highlights on the added transistors replica.

The result of this modification is a *T-structure* added on the top of the original transistor as illustrated in Fig. 7. The layout

insertions have been validated by a commercial layout editor tool configured with the FreePDK45 library design rules check. Finally, we performed the technology extraction and conversion to an H-spice model, reported in Fig. 8, using the same layout editor tool.

V. EXPERIMENTAL RESULTS

We designed two 8Kb memory modules with 1 memory bank, 256 words and 32-bits configuring the OpenRAM compiler with the original 6T-SRAM and with the developed 8T-SRAM adopting the T-structure redundant transistors. We performed two experiments evaluating the static behavior of the memory bank. The former consists on a fault injection campaign for evaluating the mitigation capability of the developed 8T-SRAM cell, the latter consists on the comparative analysis of area, leakage current and SRAM performance characteristics.

A. SEE fault injection

The fault injection simulation setup consists on modeling the SEE at the circuit level by inserting transient current sources at the impact nodes. The fault injection has been executed in two different campaigns. The former campaign measures the maximal current pulse threshold tolerated before to create the upset for each individual transistor. The latter campaign measures the dynamic sensitivity of the cell by injecting the current pulse extracted from the current pulse profile generated by the radiation analysis tool applied to the cell.

TABLE III
SRAM CELL SEE THRESHOLD CURRENT

| SRAM Configuration | SEE Threshold Current Pulse [μA] | |
|--------------------|---|-----------------------|
| | Q=1 Q _n =0 | Q=0 Q _n =1 |
| 6T-Original | 0.93 | 0.46 |
| 8T-Proposed | 3.83 | 2.12 |

In general, the most sensitive part of the SRAM inverter configuration is the drain of the n-mos transistor which is in the off stage; however, we performed the fault injection in all the transistors and we extracted the SRAM cell threshold current for creating a bit-flip within the cell. The obtained results are reported in Table III, as it possible to notice the proposed mitigated cell increases the maximal current threshold of around 4 times at the static condition Q=1 and Q_n=0 and more than 4.6 times for the condition Q=0 and Q_n=1.

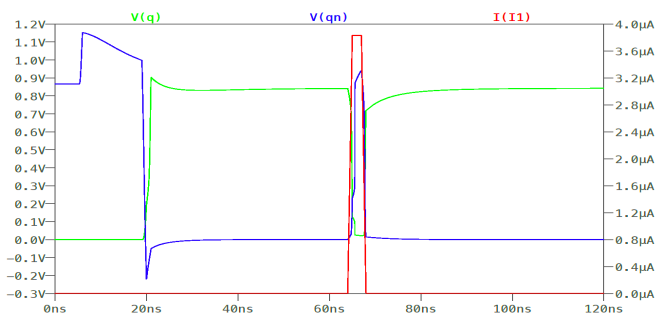


Fig. 9. An example of maximal current pulse injection pulse on the proposed 8T-SRAM cell.

A plot of the injection of the maximal current pulse for the configuration Q=1 and Q_n=0 is illustrated in Fig. 9. The injections are performed at the static storage condition of the SRAM cell and for a duration of 2ns which is 18% longer than the maximal current pulse width measured by the 3D radiation simulation. In details, the current pulse effects has a duration of around 800ps when the Q and Q_n are simultaneously at low voltage. As consequence, the two values are upset for 2.05ns. Once the current pulse expires, the original SRAM values are restored in less than 420ps.

We evaluated the overall robustness of the mitigated OpenRAM memory bank considering the radiation particle spectra described within the radiation analysis section and we performed 40,000 particle injection comparing the achieved SEE cross-section. The results, illustrated in Fig. 10, show that the developed 8TSRAM is robust more than 6 times with respect to the original cell at higher energy. Please note, that the proposed 8TSRAM is drastically more robust for low energy particles, since it is resilient more than one order of magnitude at energies below 10MeV/mgcm².

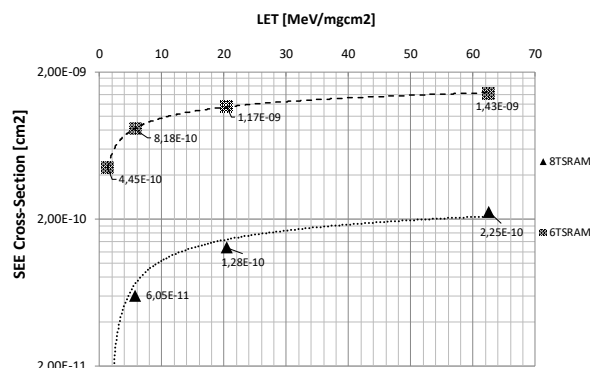


Fig. 10. The OpenRAM 8Kb memory bank SEE cross-section comparison.

B. Comparative analysis

The power dissipation, area and delay are marginally affected by the insertion of the two redundant transistors. The size of the SRAM cell is not changed by the insertion of the T-structure transistors since we included them in the original 6T-SRAM layout. However, in case of further optimization, our insertion will limit the reduction of the SRAM cell area for less than 3%.

Considering the power consumption and the functional characteristics, we compared the original and mitigated cells in order to compare the Static Noise Margin (SNM), the Read Static Noise Margin (RSNM) and the Write Static Noise Margin (WSNM). As expected, the results reported in Table IV indicates that the proposed 8T-SRAM cell is slightly degrading the leakage current while maintaining almost equivalent the SNM.

We compared the reading and writing delays characteristics of a single SRAM cell. The delay is degraded due to the additional parasitic resistive capacitive load effects that increases the average response time from 68ps up to 92ps. Finally, we also compared the standby power for the traditional 6TSRAM cell with the developed 8TSRAM observing a negligible increasing of power consumption from 6.30 μW to 6.83 μW .

TABLE IV
SRAM CELLS CHARACTERISTICS COMPARISON

| Characteristic | Original 6TSRAM | Proposed 8TSRAM |
|-----------------------------|--------------------|--------------------|
| $V_{DD}(V)$ | 1.5 | 1.5 |
| Leakage Current (μA) | 0.81 | 0.88 |
| SNM | 41.53 | 43.20 |
| RSNM | 27.40 | 38.42 |
| WSNM | 129.62 | 141.75 |

VI. CONCLUSIONS AND FUTURE WORKS

In this paper, we propose a methodology for the analysis and the mitigation of SRAM circuit generated by the open-source OpenRAM memory compiler. The main novelty of the proposed methodology is the capability to details the interaction of the radiation particle with the SRAM memory layout, to depict the sensitive transistors and to selectively mitigate the radiation effects by layout-oriented modifications. We applied the workflow methodology to the design and mitigation of the 6TSRAM cell. Thanks to the availability of the layout description provided by the OpenRAM project, we developed a new mitigation strategy to increase the current thresholds and reduce the voltage transients. An experimental analysis performed on an 8Kb memory module generated by the OpenRAM compiler demonstrates that the developed 8TSRAM-based memory module is 6 times more resilient than the original memory block at high energy particle. The resiliency is improved up to one order of magnitude at lower energies, as specifically target for ground and low earth orbit applications. We compared the functional characteristics with the original cell, and we observed a minimal deviation in leakage current and an evident improvement versus reading and writing noise margins. As future works, we plan to extend the mitigation features to other memory components and to evaluate the robustness versus destructive Single Event Latch-up (SEL) effects.

REFERENCES

- [1] B. D. Sierawski et al., "Muon-Induced Single Event Upsets in Deep-Submicron Technology," in *IEEE Transactions on Nuclear Science*, vol. 57, no. 6, pp. 3273-3278, Dec. 2010.
- [2] T. Karnik and P. Hazucha, "Characterization of soft errors caused by single event upsets in CMOS processes" *IEEE Trans. Depend. Secure Comput.*, vol. 1, no. 2, pp. 128-143, Apr.-Jun. 2004.
- [3] S. Azimi, B. Du, L. Sterpone, "On the prediction of radiation-induced SETs in flash-based FPGAs", *Microelectronics Reliability*, pp 230-234, 2016.
- [4] P. E. Dodd and L. W. Massengill, "Basic mechanisms and modeling of single-event upset in digital microelectronics" in *IEEE Transactions on Nuclear Science*, vol. 50, no. 3, pp. 583-602, June 2003.
- [5] R. Lacoé et al., "Application of Hardness-By-Design Methodology to Radiation-Tolerant ASIC Technologies", *IEEE Trans. Nuc. Sci.*, vol. 47, no. 6, pp. 2334-2341, Dec. 2000.
- [6] X. Yao, L. T. Clark, D. W. Patterson and K. E. Holbert, "Single event transient mitigation in cache memory using transient error checking circuits" *IEEE Custom Integrated Circuits Conference* 2010, San Jose, CA, USA, 2010, pp. 1-4.
- [7] M. R. Guthaus, J. E. Stine, S. Ataei, Brian Chen, Bin Wu and M. Sarwar, "OpenRAM: An open-source memory compiler," 2016 IEEE/ACM International Conference on Computer-Aided Design (ICCAD), Austin, TX, USA, 2016, pp. 1-6.
- [8] T. Ansell and M. Saligane, "The Missing Pieces of Open Design Enablement: A Recent History of Google Efforts : Invited Paper," 2020 IEEE/ACM International Conference On Computer Aided Design (ICCAD), San Diego, CA, USA, 2020, pp. 1-8.
- [9] S. Azimi, L. Sterpone, "Digital Design Techniques for Dependable High Performance Computing," IEEE International Test Conference (ITC), 2020, pp. 1-10.
- [10] S. Yoshimoto et al., "A 40-nm 0.5-V 20.1- μ W/MHz 8T SRAM with low-energy disturb mitigation scheme," 2011 Symposium on VLSI Circuits - Digest of Technical Papers, Kyoto, Japan, 2011, pp. 72-73.
- [11] R.C. Baumann and E. B. Smith, "Neutron-induced 10B fission as a major source of soft errors in high density SRAM", *Microelectronics Reliability*, Vol. 41, No. 2, pp. 211-218, February 2001.
- [12] Y.-W. Chiu et al., "40nm bit-interleaving 12T subthreshold SRAM with data-aware write-assist", *IEEE Transactions on Circuits and Systems I*, Vol. 61, pp. 2578-2688, 2014.
- [13] X. Yao, L. T. Clark, D. W. Patterson and K. E. Holbert, "Single event transient mitigation in cache memory using transient error checking circuits," *IEEE Custom Integrated Circuits Conference* 2010, pp. 1-4.
- [14] N. Seifert, M. Kirsch, "Rea-Time Soft-Error Testing Results of 45nm High-K Metal Gate, Bulk CMOS SRAMs", *IEEE Transactions on Nuclear Science*, Vol. 59, No. 6, December 2012.
- [15] J. Li, W. Chen, R. Li, G. Wang and S. Yang, "Study on Transient Ionizing Radiation Effect of 40nm SRAM", 3rd International Conference on Radiation Effects of Electronic Devices (ICREED), pp. 1-4, 2019.
- [16] K. Mohr and L. Clark, "Delay and Area Efficient First-level Cache Soft Error Detection and Correction", *IEEE ICCD Proceedings*, pp. 88-92, October, 2006.
- [17] T. Hoang, et al. "A Radiation Hardened 16-Mb SRAM for Space Applications", *IEEE Aerospace Conference*, pp. 1-6, 2006.
- [18] B. S. Mohammad, H. Saleh, M. Ismail, "Design Methodologies for Yield Enhancement and Power Efficiency in SRAM-based SoCs", *IEEE Transactions on Very Large Scale Integration (VLSI) Systems*, Vol. 23, Issue 10, pp. 2054-2064, 2015.
- [19] L. Chang et al., "An 8T-SRAM for variability tolerance and low-voltage operation in high-performance caches", *IEEE Journal of Solid-State Circuits*, Vol. 43, pp. 518-529, 2008.
- [20] I. J. Chang et al. "A 32 Kb 10T sub-threshold SRAM array with bit-interleaving and differential read scheme in 90nm CMOS", *IEEE Journal of Solid-State Circuits*, Vol. 44, pp. 650-658, 2009.
- [21] J. E. Stine et al., "FreePDK: An Open-Source Variation-Aware Design Kit", *IEEE International Conference on Microelectronic Systems Education*, pp. 173-174, 2007.
- [22] L. Sterpone, F. Luoni, S. Azimi, B. Du, "A 3-D Simulation-based Approach to Analyze Heavy Ions-Induced SET on Digital Circuits", *IEEE Transactions on Nuclear Science*, Vol. 67, Issue 9, pp. 2034 - 2041, 2020.
- [23] H. Nii et al., "A 45nm High Performance Bulk Logic Platform Technology (CMOS6) using Ultra High NA(1.07) Immersion Lithography with Hybrid Dual-Damascene Structure and Porous Low-k BEOL", *International Electron Devices Meeting*, pp. 1-4, 2006.
- [24] A. O. Akhmetov et al., "IC SEE Comparative Studies at UCL and JINR Heavy Ion Accelerators," 2016 IEEE Radiation Effects Data Workshop , Portland, OR, USA, 2016, pp. 1-4.
- [25] S. Azimi, C. De Sio, L. Sterponet., "A Radiation-Hardened CMOS Full-Adder Based on Layout Selective Transistor Duplication", *IEEE Transactions on Very Large Scale Integration (VLSI) Systems*, vol. 29, no. 8, pp. 1596-1600, 2021.